A SEMI-EMPIRICAL ALGORITHM OF WATER TRANSPARENCY AT THE GREEN WAVELENGTH BAND OF OPTICAL REMOTE SENSING

Y. Zhang, J. Pulliainen, S. Koponen, and M. Hallikainen

Helsinki University of Technology
Laboratory of Space Technology
P.O. Box 3000, FIN-02015 HUT, Finland

Abstract—This study employed water transparent characteristics from the Gulf and archipelago of Finland and the corresponding data sets of optical sensors at the green wavelength band to estimate Secchi disk depth (SDD). The SDD is one major optical measurement of water transparency in the study area, where the coastal waters are dominated by absorption from both dissolved and particulate organic matter since the Gulf is optically dominated by scattering from suspended sediments. Concurrent *in situ* measurements, Landsat TM and simulated SeaWiFS data were obtained in August 1997. The results show that the SDD from the narrow green bandwidth (20 nm) data of simulated SeaWiFS is slightly better than the SDD from the broad green bandwidth (80 nm) data of TM using the semi-empirical algorithm developed in the study. The study of water transparent characteristics in the area still needs to be further investigated using SeaWiFS, MODIS and MERIS in the future.

1. INTRODUCTION

The use of satellite imagery for water quality mapping started as early as 1973 with the work by Klemas, Bowker and Ruggles. All three authors reported in the Symposium on Significant Results Obtained from ERTS-1 data (Earth Resources Technology Satellite, later renamed Landsat-1). Up to now, the digital evaluation of satellite information at visible and near infrared (NIR) wavelengths has been used to estimate water quality parameters [1–5]. Observations of Secchi disk depth, turbidity and suspended sediment concentration provide quantitative information concerning water quality conditions and can be used in various numerical schemes to help characterize the trophic state of an aquatic ecosystem [6]. However, *In situ* measurements of water quality characteristics tend to be limited, especially in the temporal and spatial domains, because of the costs associated with data collection and laboratory analysis. Present and future sensors such as Landsat TM, AVHRR, SeaWiFS, MODIS and MERIS can provide an alternative means for obtaining relatively low-cost, simultaneously information on surface water conditions from numerous lakes and coastal or oceanic areas situated within a large geographic area [7–15].

Secchi disk depth (SDD) is one important optical measurement of water quality and differs from suspended sediment concentration for example, which is a measure of the weight of inorganic particulates suspended in the water column [10, 16]. So far the SDD has become the universally accepted tool to measure water transparency [17–21]. Water quality in the form of the water transparency in the visual region is very important for hydro-optical application [22]. Although there have been many efforts to map this variable from satellite imagery, the results for individual scenes to derive water surface parameters are not very consistent [11].

The Gulf of Finland is optically dominated by scattering from suspended sediments, whereas the coastal waters of the Gulf and coastal archipelago are dominated by absorption from both dissolved and particulate organic matter. This is because the Gulf and archipelago of Finland is highly affected by the input from the rivers that discharge a high concentration of mineral suspended solids and nutrients. The optical characteristics of the water have been studied by using space-borne and aircraft borne remotely sensed data in the Gulf of Finland [23–26]. In this study, however, we present a semi-empirical algorithm of the SDD using the green wavelength band of Landsat TM and simulated SeaWiFS data in the Gulf and coastal archipelago of Finland in August 1997.

2. STUDY AREA AND IN SITU DATA

The Gulf of Finland is strongly eutrophied because of the anthropogenic nutrient load. The eutrophication problem of the Gulf has been studied [27]. The Gulf of Finland is relatively shallow, with a mean depth of 38 m and a maximum depth of 123 m. The total water volume is about 1,130 km^3. The surface area (29,600 km^2) is small compared with the catchment area (421,000 km^2). The incoming river discharge is about 110 km^3/year. In the easternmost part of the Gulf the salinity is very low because of the fresh water of the River Neva. The average salinity on the surface is close to 0.6% in December and 0.3–0.6% in June. The Gulf is also saline stratified and in summer temperature stratified. Ecologically, most of the Gulf is nitrogen limited, but that the inner Neva estuary is phosphorus limited [27]. Therefore, the factors causing increased light attenuation (organic matter, phytoplankton, and suspended sediments) vary temporally as well as spatially.

Concurrent *in situ* measurements of water transparency, Landsat TM and simulated SeaWiFS data were collected in August 1997 in the study area.

3. LANDSAT TM AND SIMULATED SEAWIFS DATA

3.1. Landsat TM Data

When optical sensors data, transformed into radiances as seen by the satellite, are used to retrieve quantitative data concerning the Earth's surface, a procedure to correct the measured radiance for the atmospheric contribution is required. The remaining amount of radiance that reaches the sensor (water leaving radiance) can range from 25% at the blue region of electromagnetic spectrum to 0% at the near infrared (NIR) region [4]. One technique over water areas is to observe a reflectance target such as deep, clear water, a "dark object" [28], that should almost completely absorb all light in the NIR wavelength region, and thus should have brightness values close to zero [29].

In this study, one scene of Landsat TM data was acquired on 16th August 1997. The resolution of TM data is 30 meters (except band 6 with 120 meters). Since the TM data was only one scene in the study area, the atmospheric correction of TM was ignored for the purpose of correlation analysis [30, 31]. However, the TM image was geometrically corrected using the landuse map, and then the land area of the image was masked off. In order to extract the TM bands data from those ground truth points (water quality sampling stations), the mean and

standard deviation of TM digital number values were calculated using the defined windows of 300 by 300 meters for each ground truth point.

3.2. Simulated SeaWiFS Data

For the purpose of comparison between different optical sensors during the same campaign, simulated SeaWiFS data were resampled from the Airborne Imaging Spectrometer for Applications (AISA) [32] data on 14th August 1997. The data were spatially and temporally averaged corresponding to the characteristics of the SeaWiFS sensor. That is, the spatial resolution is 1.1 km and the central wavelengths should only be at 490 nm, 510 nm, 555 nm, 670 nm, and 765 nm (AISA excluded 412 nm and 443 nm due to its range at 450–900 nm). Similarly, the simulated SeaWiFS data were extracted corresponding to those ground truth points by the defined boxes of 1.1 by 1.1 km for each ground truth point.

4. A SEMI-EMPIRICAL ALGORITHM

Many retrieval algorithms in literature are based on some logarithmic relation of the reciprocal of the SDD [11]. In this study, however, we developed a semi-empirical algorithm of SDD using the green wavelength band of Landsat TM data and simulated SeaWiFS data over the Gulf and coastal archipelago of Finland.

Secchi disk depth (SDD) for monochromatic light can be given by [33]

$$SDD = 6.3/c \qquad (1)$$

where c is the attenuation coefficient. The Secchi disk [33] was viewed through a series of blue, green and red filters with matching filters used in a transmissometer for the attenuation coefficient measurements. For turbid waters, the main contribution to attenuation comes from scattering, and c is independent of wavelength, to a good approximation [34]. Therefore, Equation (1) would be a good approximation for the naked eye, without filters [21].

Attenuation, backscattering and absorption coefficients can be further expanded as

$$
\begin{align}
c &= c_p + c_w + c_s & (2a)\\
b_b &= b_{bp} + b_{bw} + b_{bs} & (2b)\\
a &= a_p + a_w + a_s & (2c)
\end{align}
$$

where subscripts p, w, and s refer to contributions from particles, pure sea water and dissolved substance, respectively. Also, $b_{bw} = 0.5b_w$, where b_w is the scattering coefficient for pure sea water [35].

In the Gulf of Finland, the coastal water is predominantly green to blue-green in color, except in the plumes of rivers after heavy rain, so that a submerged Secchi disk can be seen at a central wavelength of the green band. This is very similar to the central wavelength (560 nm) of Landsat TM band 2 (i.e., 520–600 nm) and the central wavelength (555 nm) of SeaWiFS band 5 (i.e., 545–565 nm), respectively. For the green band it is reasonable to consider that the effects of dissolved substances are negligible [35]. In this band, the absorption by phytoplankton can also be assumed as a minimum [36]. Therefore, we can suppose that all particles are purely scatterers, i.e., their absorption is negligible in this band, i.e., $a_p \ll a_w$ [21]. Then we can get

$$c = c_p + c_w \tag{3a}$$

$$b_b = b_{bp} + 0.5b_w \tag{3b}$$

$$a = a_w \tag{3c}$$

On the other hand, remote sensing reflectivity (R) can be given by [4]

$$R = 0.33b_b/a \tag{4}$$

where R is the ratio of upwelling to downwelling irradiance just below the sea surface, b_b is the backscatter coefficient, and a is the absorption coefficient.

Therefore, Equation (4) becomes as follows using Equations (3b) and (3c)

$$R = 0.33(b_{bp} + 0.5b_w)/a_w \tag{5}$$

where R is now remote sensing reflectivity at the green band. Let us put $b_{bp} = Bb_p = Bc_p$, where B is the ratio of backscatter to total scattering coefficient for particles, then Equation (5) becomes

$$R = 0.33(Bc_p + 0.5b_w)/a_w \tag{6}$$

From Equation (1) with $c = c_p + c_w$, thus

$$c_p = 6.3/SDD - c_w \tag{7}$$

and then further

$$R = 0.33(B(6.3/SDD - c_w) + 0.5b_w)/a_w \tag{8}$$

Now, we note that B is the only adjustable constant in Equation (8). The theoretical value for pure water is 0.5. Values for coastal water appear to range between 0.006 and 0.025 [21]. In literature for the ratio of backscatter to total scattering coefficient for ocean waters

(not just for particles), the value ranges between 0.006 and 0.11 [36, 37]. In fact, to develop Equation (8), we have assumed that $c_p \gg c_w$ and $(6.3B/SDD) \gg 0.5b_w$. Therefore, given a value for B of approximately 0.01 and then putting $c_w = 0.066\,\mathrm{m^{-1}}$ and $b_w = 0.002\,\mathrm{m^{-1}}$ [33], both these inequalities will be satisfied if $SDD \ll 100\,\mathrm{m}$, which is always true in coastal waters [21]. Then, Equation (8) becomes

$$R = 0.33(6.3B/SDD)/a_w \tag{9}$$

and with $a_w = 0.064\,\mathrm{m^{-1}}$ [33], therefore

$$1/SDD = (0.031/B)R \tag{10}$$

5. RESULTS AND DISCUSSION

Our previous examination of the correlation matrix among TM band 1–7 digital values showed that the correlations (r^2) for TM band 1–7 pairs ranged between 0.001 and 0.933. This difference among all the bands implies that the blue wavelength band (TM1), green wavelength band (TM2), red wavelength band (TM3), and NIR wavelength band (TM4), as well as middle and thermal infrared wavelength bands (TM5, TM6 and TM7) either changed significantly at any site or changed differently at all sites. This probably have a significant effect on results of data analysis in the study area [38].

The previous examination also indicated that SDD had a correlation (r^2) of 0.31 with chlorophyll-a and that (r^2) of 0.49 with suspended sediment concentration. This means that the SDD has significant relationships with both organic and inorganic matters in the study area [39].

Using Equation (10), the SDD estimated from the TM2 is plotted against the SDD measured *in situ* shown in Figure 1, in which the coefficient of determination $R^2 = 0.51$ and the adjustable constant $B = 0.0167$. In the same way, the coefficient of determination of SDD from the green band of simulated SeaWiFS is $R^2 = 0.53$.

We also found that there would be a better result for the data set of SDD at the range between 0.67 m and 2.7 m using equation (10) from the TM2. The coefficient of determination $R^2 = 0.67$ and the adjustable constant $B = 0.0173$ (Figure 2) with root mean square error (RMSE) of 0.36 m. Similarly, for the same range of SDD, the coefficient of determination from the green band of simulated SeaWiFS is $R^2 = 0.71$ with $RMSE = 0.30\,\mathrm{m}$ (Figure 3).

In the international literature the mapping of SDD has shown similar results. The results for individual scenes are not very consistent and show variability from 0.59 to 0.98 [11]. In practice, however, the
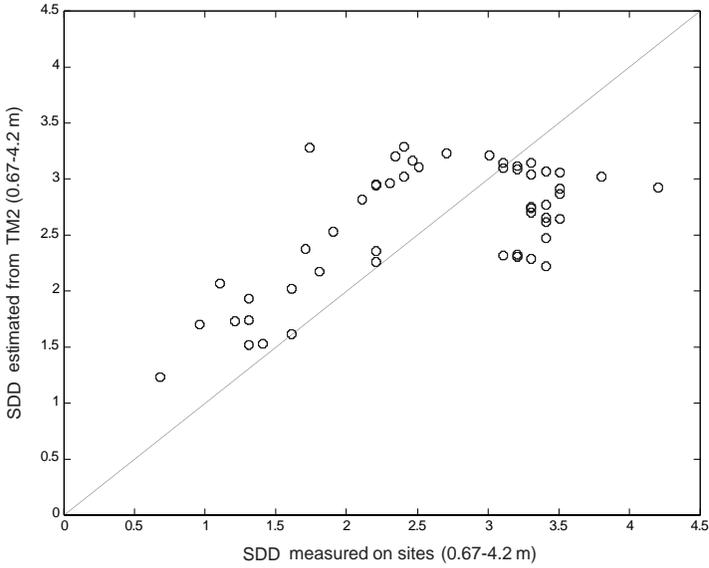
Figure 1. Regression of SDD measured with estimated (0.67–4.20 m) from TM2 using the semi-empirical algorithm.
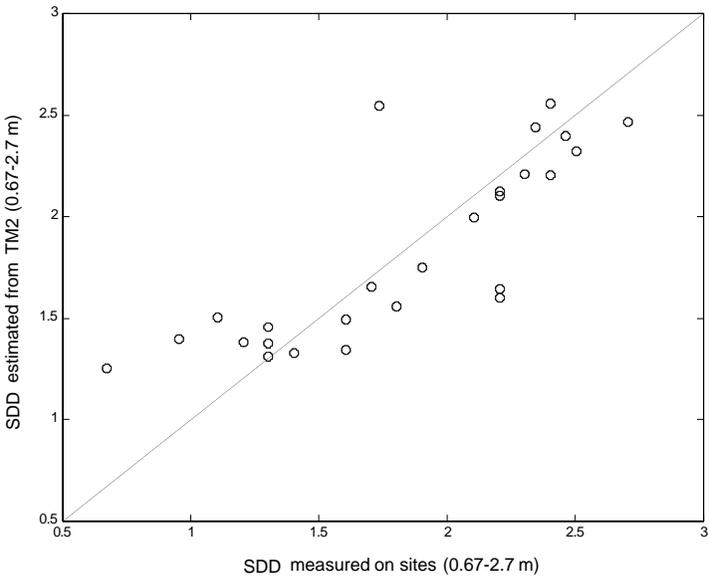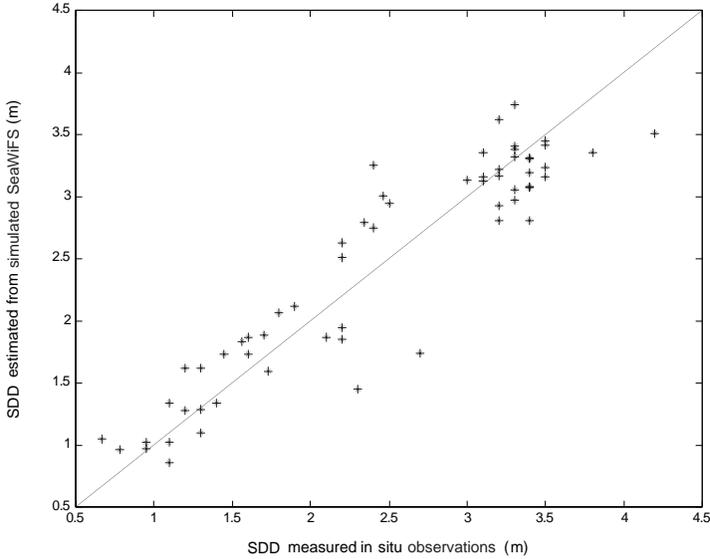

Figure 2. Regression of SDD measured with estimated (0.67–2.70 m) from TM2 using the semi-empirical algorithm.
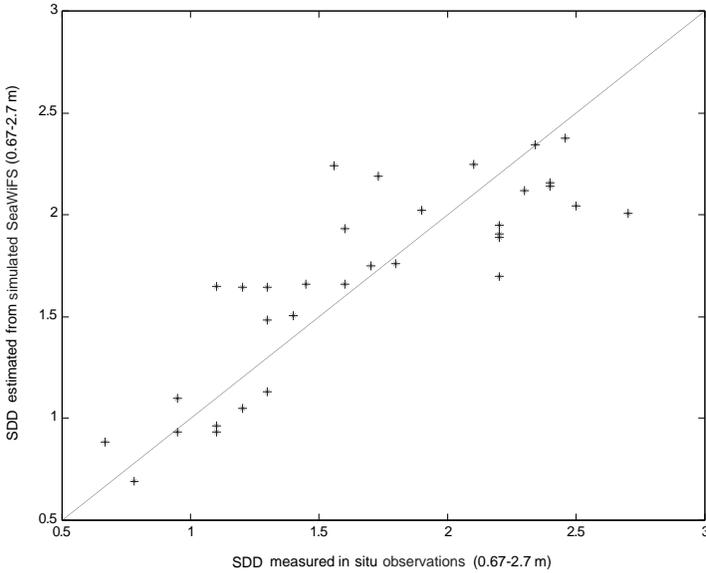
Figure 3. Regression of SDD measured with estimated (0.67–2.70 m) from simulated SeaWiFS band5 using the semi-empirical algorithm.

results from this semi-empirical algorithm are not so good as those from the multivariate regression analysis using all TM visible bands in our previous studies [30, 31]. Table 1 presents the comparison of the results using the semi-empirical approach and our previous results using the multivariate regression analysis. The results indicate that the visible bands of TM data [30] and simulated SeaWiFS data have the greatest ability to estimate SDD using multivariate algorithms. The results were estimated from the TM visible bands ($R^2 = 0.72$ and $RMSE = 0.45$ m) and from the availably simulated SeaWiFS visible bands ($R^2 = 0.86$ and $RMSE = 0.34$ m shown in Figure 4) at the range between 0.67 m and 4.2 m. This probably indicates that the narrow bandwidth of optical sensors is more critical than their spatial resolution to estimate SDD. However, if these multivariate algorithms were applied to the range between 0.67 m and 2.7 m, both results are almost same ($R^2 = 0.80$ or 0.81 and $RMSE = 0.24$ m seen in Table 1). The probable reason of this difference and similarity still needs to be further investigated in our future studies.

Although, in practice, this semi-empirical algorithm developed in the study is not adequately good to estimate the SDD, it is still very useful to detect changes of SDD in the study area. Therefore, the semi-empirical algorithm of water transparency in the area still needs

Figure 4. Regression of SDD measured with estimated (0.67–4.20 m) from simulated SeaWiFS visible bands using the multivariate algorithm.

Table 1. Comparison of results from the semi-empirical and multivariate algorithms.

R^2 (RMSE)	Semi-empirical	Semi-empirical	Multivariate	Multivariate
SDD range	0.67-4.20 m	0.67-2.70 m	0.67-4.20 m	0.67-2.70 m
Landsat TM	0.51 (0.68 m)	0.67 (0.36 m)	0.72 (0.45 m)	0.80 (0.24 m)
Simulated SeaWiFS	0.53 (0.64 m)	0.71 (0.30 m)	0.86 (0.34 m)	0.81 (0.24 m)

to be further refined and applied in the future using present and near new coming optical sensors such as SeaWiFS, MODIS and MERIS.

6. CONCLUSIONS

In this study, we present one semi-empirical algorithm to estimate SDD through a case study in the Gulf and archipelago of Finland. The water transparency information and the corresponding data sets of Landsat TM and simulated SeaWiFS were used in the study area. The TM and simulated SeaWiFS data from locations of water samples were extracted and digital data were examined. Significant correlations were observed between digital data and SDD observations. Although

the SDD estimated accuracy is not adequately good, the results still support our previous studies. We also found that, for the SDD range between 0.67 m and 2.7 m, the best result estimated from the green band of Landsat TM is $R^2 = 0.67$ and $RMSE = 0.36$ m, whereas the best one from the green band of simulated SeaWiFS is $R^2 = 0.71$ and $RMSE = 0.30$ m.

The results also show that the narrow bandwidth data of the optical remote sensor is more critical than its spatial resolution for the purpose of estimating SDD from optical remote observations. The further study of water transparent characteristics in the area will be investigated in the future using present and near coming optical sensors such as SeaWiFS, MODIS and MERIS.

ACKNOWLEDGMENT

REFERENCES

1. Alföldi, T. and J. C. Munday, "Water quality analysis by digital chromaticity mapping of Landsat data," *Canadian J. Remote Sens.,* Vol. 4, 108–122, 1978.

2. Moore, G. K., "Satellite remote sensing of water quality," *Hydrol. Sci.,* Vol. 25, 407–421, 1980.

3. Austin, R. W. and T. J. Petzold, "Water color measurements," *Oceanography from Space,* J. F. R. Gover (ed.), 239–256, New York, 1981.

4. Gordon, H. R. and A. Y. Morel, *Remote Assessment of Ocean Color for Interpretation of Satellite Imagery — A Review,* Spring-Verlag, New York, 1983.

5. Ferrari, G. M., N. Hoepffner, and M. Mingazzini, "Optical properties of the water in a deltaic environment: prospective tool to analyze satellite data in turbid waters," *Remote Sens. Environ.,* Vol. 58, 69–80, 1996.

6. Carlson, R. E., "A trophic state index for lakes," *Limnol. Oceanogr.,* Vol. 22, 361–369, 1977.

7. Carpenter, D. S. and S. M. Carpenter, "Monitoring inland water quality using Landsat data," *Remote Sens. Environ.,* Vol. 13, 345–352, 1983.

8. Tassan, S., "Evaluation of the potential of the Thematic Mapper for marine application," *Int. J. Remote Sens.,* Vol. 8, 1455–1478, 1987.

9. Doerffer, R., J. Fischer, M. Stossel, and C. Brockmann, "Analysis of Thematic Mapper data for studying the suspended matter distribution in the coastal area of the Germany Bight (North Sea)," *Remote Sens. Environ.,* Vol. 28, 61–73, 1989.

10. Harrington, J. A., Jr. and F. R. Schiebe, "Remote sensing of Lake Chicot, Arkansas: monitoring suspended sediments, turbidity, and secchi depth with Landsat MSS data," *Remote Sens. Environ.,* Vol. 39, 15–27, 1992.

11. Lindell, T., D. Pierson, G. Premazzi, and E. Zilioli, *Manual for Monitoring European Lakes Using Remote Sensing Techniques,* (Luxembourg: Official Publications of the European Communities), EUR 18665 EN, 1999.

12. McClain, C. R., M. L. Cleave, G. C. Feldman, W. W. Gregg, and S. B. Hooker, "Science quality SeaWiFS data for global biosphere research," *Sea Tech.,* Vol. 39, 10–16, 1998.

13. Schiller, H. and R. Doerffer, "Neural network for emulation of an inverse model-operational derivation of Case II water properties from MERIS data," *Int. J. Remote Sens.,* Vol. 20, 1735–1746, 1999.

14. Woodruff, D. L., R. P. Stumpf, J. A. Scope, and H. W. Paerl, "Remote estimation of water clarity in optically complex estuarine waters," *Remote Sens. Environ.,* Vol. 68, 41–52, 1999.

15. Ruddick, K. G., F. Ovidio, and M. Rijkeboer, "Atmospheric correction of SeaWiFS imagery for turbid coastal and inland waters," *Appl. Opt.,* Vol. 39, 897–912, 2000.

16. Schiebe, F. R., J. A. Harrington, and C. B. Ritchie, "Remote sensing of suspended sediments: the Lake Chicot, Arkansas project," *Int. J. Remote Sens.,* Vol. 13, 1487–1509, 1992.

17. Lathrop, R. G., T. M. Lillesand, and B. S. Yandell, "Testing the utility simple multi-date Thematic Mapper calibration algorithms for monitoring turbid inland waters," *Int. J. Remote Sens.,* Vol. 12, 2045–2063, 1991.

18. Mausel, P. W., M. A. Karakaka, C. Y. Mao, D. E. Escobar, and J. H. Everitt, "Insights into secchi transparency through computer analysis of aerial multispectral video data," *Int. J. Remote Sens.,* Vol. 12, 2485–2492, 1991.

19. Dekker, A. G. and S. W. M. Peters, "The use of the Thematic Mapper for the analysis of eutrophic lakes: a case study in the

Netherlands," *Int. J. Remote Sens.,* Vol. 14, 799–821, 1993.

20. Lavery, P., C. Pattiaratchi, A. Wyllie, and P. Hick, "Water quality monitoring in estuarine water using the Landsat Thematic Mapper," *Remote Sens. Environ.,* Vol. 46, 268–280, 1993.

21. Mulhearn, P. J., "Landsat reflectivities versus secchi disc depths," *Int. J. Remote Sens.,* Vol. 16, 257–268, 1995.

22. Lindell, L. T., O. S. M. Jonsson, and T. H. Claesson, "Mapping of coastal water turbidity using Landsat imagery," *Int. J. Remote Sens.,* Vol. 6, 643–656, 1985.

23. Eloheimo, K., T. Hannonen, P. Härmä, T. Pyhälahti, S. Koponen, J. Pulliainen, and H. Servomaa, "Coastal monitoring using satellite, airborne and *in situ* data in the archipelago of Baltic Sea," *Proceed. 5th Int. Conference Remote Sens. Marine and Coastal Environ.,* San Diego, USA, Oct. 5–7, 1998.

24. Hallikainen, M., "Development of sensors and methods for remote sensing of northern areas by HUT laboratory of space technology," *IEEE Geosci. Remote Sens. Newsletter,* ISSN 0161-7869, Vol. 107, 10–11, Dec. 1999.

25. Pulliainen, J., K. Gallio, K. Eloheimo, S. Koponen, et al., "A semi-operational approach to water quality retrieval from remote sensing data," *The Science of the Total Environment,* Vol. 268, 79–93, 2001.

26. Koponen, S., J. Pulliainen, H. Servomaa, Y. Zhang, M. Hallikainen, K. Gallio, et al., "Analysis on the feasibility of multi-source remote sensing observations for chl-a monitoring in Finnish lakes," *The Science of the Total Environment,* Vol. 268, 95–106, 2001.

27. Kuusisto, M., J. Koponen, and J. Sarkkula, "Modelled phytoplankton dynamics in the Gulf of Finland," *Enviorn. Modelling and Software.,* Vol. 13, 461–470, 1998.

28. Chavez, P. S. Jr., "An improved dark-object subtraction technique for atmospheric scattering correction of multispectral data," *Remote Sens. Environ.,* Vol. 24, 459–479, 1988.

29. Gilabert, M. A., C. Conese, and F. Maselli, "An atmospheric correction method for the automatic retrieval of surface reflectances from TM images," *Int. J. Remote Sens.,* Vol. 15, 2065–2086, 1994.

30. Zhang, Y., J. Pulliainen, S. Koponen, and M. Hallikainen, "Applicability of combined microwave and optical data for surface water quality retrievals," *J. of Electromagn. Waves and Appl.,* Vol. 16, 249–251, 2002.

31. Zhang, Y., J. Pulliainen, S. Koponen, and M. Hallikainen, "Application of an empirical neural network to surface water quality estimation in the Gulf of Finland using combined optical and microwave data," *Remote Sens. Environ.,* Vol. 81, 327–336, 2002.

32. Mäkisara, K., M. Meinander, M. Rantasuo, J. Okkonen, M. Aikio, K. Sipola, P. Pylkkö, and B. Braam, "Airborne imaging spectrometer for applications (AISA)," *Digest of IGARSS'93,* Vol. 2, 479–481, Tokyo, Japan.

33. Hojerslev, N. K., "Optical properties of sea water," *Oceanography, Subvolume a of Landbolt-Bornstein Numerical Data and Functional Relationships in Science and Technology, Group V Geophysics and Space Research,* J. Sundermana (ed.), Vol. 3, Section 3.3, Spring-Verlag, London, 1986.

34. Phillips, D. M. and J. T. O. Kirk, "Study of the spectral variation of absorption and scattering in some Australia coastal waters," *Australia J. Marine and Freshwater Res.,* Vol. 34, 635–644, 1984.

35. Jerlov, N. G., *Marine Optics,* Elservier, Amsterdam, 1976.

36. Shifrin, K. S., *Physical Optics of Ocean Water,* American Institute of Physics, New York, 1988.

37. Mankovskiy, V. I., "Spectral variability of the coefficient of asymmetry of the light scattering function by sea water," *Oceanology,* Vol. 24, 46–51, 1984.

38. Zhang, Y., S. Koponen, J. Pulliainen, and M. Hallikainen, "Landsat Thematic Mapper (TM) data analysis for chlorophyll-a and turbidity in Finland Gulf," *URSI/Remote Sensing Club of Finland/IEEE XXIII Convention on Radio Science and Remote Sensing Symposium,* 69–70, Finland, August 24–25, 1998.

39. Zhang, Y., S. Koponen, J. Pulliainen, and M. Hallikainen, "Turbidity and Secchi disk depth analysis derived from Landsat Thematic Mapper data combined with ERS-2 data in the Gulf of Finland," *The 2nd Int. Symposium Operationalization of Remote Sensing,* ITC, The Netherlands, August 16–20, 1999 (CD ROM).